POLITECNICO DI TORINO
Repository ISTITUZIONALE

Development of the H4C Model of Quench Propagation in the ENEA HTS Cable-In-Conduit Conductor

(Article begins on next page)

29 November 2022

Development of the H4C model of quench propagation in the ENEA HTS Cable-In-Conduit Conductor

A. Zappatore, A. Augieri, R. Bonifetto, G. Celentano,
M. Marchetti, A. Vannozzi and R. Zanino *Senior Member, IEEE*

Abstract—**Experiments on quench propagation in high-current, high field High Temperature Superconducting (HTS) Cable-In-Conduit Conductors (CICCs) for fusion applications are forthcoming. Among the conductor designs to be tested, there is the ENEA slotted core proposal. In order to support the design of the samples and plan the diagnostics to be employed, a 1D multi-region thermal-hydraulic and electric model of the samples has been developed using the H4C code. After an experimental electric characterization, the model is applied to the simulation of quench propagation in the samples. The simulations show how current redistributes among the tapes and the slots. Additionally, they show that the quench protection strategy is suitable to prevent too high hot-spot temperatures.**

Index Terms—**High temperature superconductors, cable-in-conduit conductors, thermal-hydraulic-electric modeling, quench**

I. INTRODUCTION

HIGH Temperature Superconductors (HTS) are being investigated worldwide for many applications, such as nuclear fusion [1], particle accelerators [2], power devices [3], energy storage [4] and magnetic resonance imaging [5]. In the case of nuclear fusion, several Cable-in-Conduit Conductor (CICC) designs are being proposed [6]. Different strategies to assemble the tapes and/or the stacks in the conductor are being proposed and tested, such as:

- wrapping the tapes around a copper core [7];
- inserting [8] or enclosing [9] the stacks each in a copper tube;
- placing the stacks in the slots of a (twisted) bulky aluminum core [10].

The latter seems to be the most promising manufacturing technique, based on the Twisted-Stacked-Tape Cable, firstly proposed in [11], as it is the principle of several CICC designs [6]. The basic idea is to pile few tens of Rare-Earth Barium Copper Oxide (REBCO) tapes up to form a so-called stack. In order to reach the few tens of kA needed for fusion-grade magnets, few stacks are assembled together (in an electric parallel) in the same cable. The latter is then inserted in an aluminum jacket in order to provide mechanical robustness and confinement for the coolant, which is typically supercritical helium at 4.5 K. The stacks are then usually twisted to reduce AC losses

[11]. The conductor idea is therefore that of the CICC, already widely employed in Low Temperature Superconducting (LTS) magnets [12].

The design of fusion magnets based on HTS conductors is currently ongoing worldwide [13], [14], [15]. However, the behavior of such conductors in conditions such as quench propagation has not been fully explored yet. This strongly motivates both numerical modelling investigations and experimental campaigns.

Concerning the experimental activity, a first extensive experimental campaign is currently ongoing within the EUROfusion framework [16], with the aim of studying the quench propagation of several CICC designs at high current and high field.

On the other hand, the numerical modelling effort on quench in HTS CICCs has recently started, see for example [17], [18] and [19]. The different material properties and geometry of HTS with respect to LTS CICCs have remarkable implications on the modeling approach of the former, especially in the case of fast transients like a quench [20].

In this work, we focus on the modelling of the ENEA HTS CICC samples during quench. Whereas a first quench analysis on the full ENEA conductor was presented in [21], a dedicated and more detailed model is needed, in order to:

- support the design of the samples to be tested
- design the thermal and electric diagnostics
- have a tool to interpret the experimental results

The development of such a model, together with the necessary experimental conductor characterization, and its application to the quench in three different sample configurations are presented here.

The paper is organized as follows: after a brief description of the SULTAN operating conditions and of the sample layouts, the experimental conductor characterization is presented, together with the model employed in the numerical analyses. The results, in terms of thermal and electric behavior of the conductor samples during the quench, are discussed.

TABLE I
SULTAN OPERATING CONDITIONS

Maximum current [kA]	15
Maximum magnetic field [T]	10.9
He inlet (maximum) temperature [K]	4.5 (15)
He inlet pressure [bar]	6
He mass flow rate [g/s]	5
Discharge time constant [s]	0.1
Detection time delay [s]	0.5

Fig. 2. (a) Picture and (b) cross-section of the ENEA HTS CICC short sample used for the electrical characterization. (c) Measured electric resistance between tapes - numbered as in (b) - in the same and in different slots.

II. THE ENEA HTS CICC SAMPLES

The ENEA HTS CICC samples are planned to be tested in SULTAN [22], whose main operating conditions are reported in Table I.

Some of the sample design options are sketched in Fig. 1. They all have ~ 80 tapes in total (rather than 120, as in the full-size conductor), in order to comply with the SULTAN maximum current. They differ either in terms of orientation of the HTS stacks with respect to the magnetic field, see C1 and C2 in Fig. 1, or in the number of tapes per slot, see C3 in the same figure. This leads to a different current sharing temperature (T_{CS}), i.e. the temperature at which the operating current is equal to the critical current, see Table II. Note that T_{CS} in each tape in C3 is slightly lower than in C1 because the number of tapes is lower (78 in C3, 80 in C1 and C2), leading to a higher current per tape, since the total current is kept constant and equal to 15 kA.

All samples will be cooled with supercritical He flowing only in the central channel. To ensure leak tightness, an additional stainless steel jacket will be probably employed. The slots will not be twisted to greatly facilitate the manufacturing of the samples as well as the positioning of all the sensors on and inside the samples.

The quench will be induced increasing the He inlet temperature up to 15 K.

III. ELECTRIC CHARACTERIZATION OF THE CICC

A short sample (~ 50 cm) of the CICC has been electrically tested at 77 K in its self-field at ENEA Frascati, in order to measure the inter-tape and inter-slot electrical resistances. The resistance between two adjacent tapes X and Y of the same stack was measured connecting tape X to a bus-bar on one end of the CICC and tape Y to the other bus-bar on the opposite end

of the sample. To measure the resistance between two adjacent slots, tape X in slot A and tape Y in slot B are connected to the two bus-bars, see Fig. 2.

The average value of the measured inter-tape and inter-slot electric resistance is 5 μΩ/m and 50 μΩ/m, respectively. These values were adopted in the numerical model, see Section IV.

The inter-tape resistance is quite uniform within each slot (except between the first two innermost tapes, probably because they are pressed more than the other, leading to a lower contact resistance).

The measured value of the inter-slot resistance depends on which pair of tapes is chosen to be connected to the bus-bars, because also the inter-tape resistance is included in the measurement. Indeed, keeping the A20 tape fixed and moving upwards in slot B, i.e., from B18 to B1, the total measured resistance gradually increases, as expected, because the inter-tape resistances among the tapes of stack B pile up on top of the inter-slot resistance between stacks A and B.

IV. NUMERICAL MODEL

The H4C code [18] solves, along the conductor axis, (1) a 1D heat conduction equation for each thermal (solid) region, (2) a set of Euler-like equations for the speed, pressure and temperature of the coolant for each fluid region and (3) a diffusion-like equation for the current distribution in each electric region, being the number of solid, fluid and electric regions arbitrary.

In this work, the H4C model of the ENEA samples is based on the detailed electro-thermal model presented in [21]. In [21]
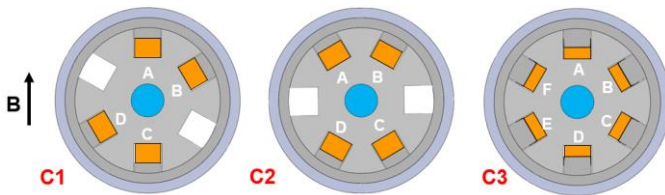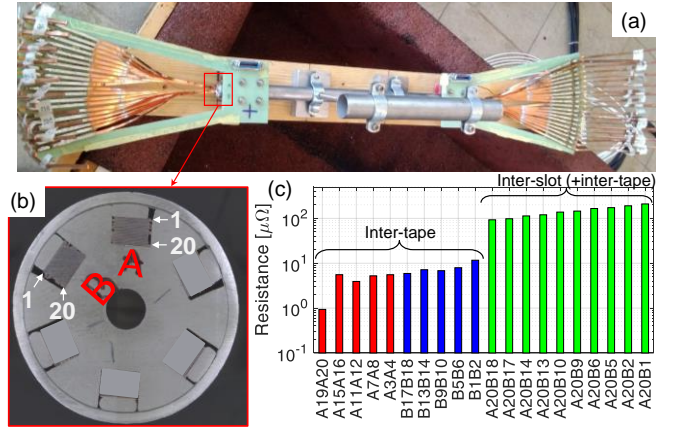

Fig. 1. Cross section of the samples under investigation. The stacks are colored in orange; the aluminum core, jacket and fillers on top of the stacks are colored in grey; the central channel, where He flows, is colored in light blue; the external stainless steel jacket is colored in light purple; the white slots are empty. The direction of the external SULTAN magnetic field is also shown.

TABLE II
CHARACTERISTICS OF THE SAMPLES

Tapes per slot, C1 [-]	20
Tapes per slot, C2 [-]	20
Tapes per slot, C3 [-]	13
&$T_{CS,C1}$ [K]	8.8, 20.9
$T_{CS,C2}$ [K]	11.6
&$T_{CS,C3}$ [K]	8.0, 20.1

&The different value of T_{CS} in the same configuration is due to the corresponding orientation with respect to the magnetic field

it was shown that, if the cross-section of a slot is lumped in a single electric and thermal region, the error on the temperature increase during the quench propagation can be up to 15 %. Therefore, in order to have a more accurate description of the relevant quantities, e.g. the hot-spot temperature reached during the transient, as well as an insight on the current redistribution among the tapes (and the slots), each tape is described here by a single electric and thermal region. This leads to ~ 80 electric and thermal regions per each conductor sample. A single fluid region is used to simulate the He flow in the central channel. The friction factor is computed according to the Petukhov correlation [25], which gives $f_{Blasius} = 0.012$ before quench initiation.

The interfaces among the different regions are modelled in the following way:

- Tape-Tape
  - Thermal contact resistance equal to 0.5 m^2 K / W [23];
  - Electrical contact resistance from measurements, see Section III;
- Tape-Core
  - Thermal contact resistance equal to 0.6 m^2 K / W [24];
  - Electrical contact resistance from measurement, see Section III;
- Fluid-Core

  - Heat transfer coefficient from Dittus-Boelter correlation [25], which, before the quench initiation is ~ 2160 W / m^2 / K.

The scaling law of the superconductor is based on [17]. The angular dependence of the critical current density J_C is taken into account through the Ginzburg-Landau law [19].

The inductance matrix has been computed using the definition of the (mutual) inductance $M_{12} = \frac{\mu_0}{4\pi S_1 S_2} \int_{V_1} \int_{V_2} \frac{1}{r_{12}} dV_1 dV_2$, where "1" and "2" are two general tapes, μ_0 is the vacuum permeability, S_1, S_2, V_1 and V_2 are the cross-sectional area and volume of tape 1 and 2 and r_{12} is the relative distance between the two infinitesimal volumes dV_1 and dV_2. The integration has been performed numerically using a simple script developed in Matlab and benchmarked against the analytical solution shown in [26]. The inductive effect of the core has been neglected for simplicity and because it is not expected to play an important role on the short time scales due to its high electric resistance with respect to the copper and, a fortiori, to the HTS before the full transition to the normal state.

The inductance values used in the model between the tapes (in C1) are the following:
- in the same slot: from 4.9 μH (self-inductance) to 3.9 μH
- in slot A and B: from 3.6 μH to 3.2 μH
- in slot A and C: from 3.1 μH to 2.8 μH
- in slot A and D: from 3.3 μH to 3.0 μH
Very similar values are obtained for C2 and C3.

The boundary conditions of the equations being solved are the following: adiabatic ends for the temperature in the solids; imposed inlet and outlet pressure and inlet temperature for the fluid model equations; imposed current in each tape at one end of the conductor and zero current gradient, i.e., null voltage, at the other end. The initial conditions are the following: uniform temperature in both solids and fluids, linear pressure distribution from inlet to outlet and uniform speed. The current at t = 0 s is assumed to be equally distributed among all the superconducting tapes and it is dumped, according to the values reported in Table I, when 100 mV are reached on the full sample length.

V. RESULTS

In this Section, the results obtained with the H4C model of the ENEA HTS samples are presented.

First, the evolution of the quench is discussed, focusing on the C1 sample. Then, the comparison of the quench evolution in the three samples is presented.

A. Quench in C1

1) Current evolution

The current evolution in stack A and B of C1 is shown in Fig. 3. Since the warm helium is heating the core, all the stacks are heated up in the same way until the current starts to be shared among the tapes. The current starts redistributing at t ~ 0.8 s: the current from the tapes at the bottom of stack A, which are heating up, passes to the top tapes of the same stack, as they are colder, and can still carry most of the current of the stack. At t ~ 0.87 s, the tapes enter the current-sharing state, see the rise of the current in the tape stabilizers in Fig. 3(a). At the same time, part of the current starts flowing away from stack A, see Fig. 3(b), going back from the top to the bottom tapes.

The current of stack A is then shared between the core and stack B (the same is true for stacks C and D, as they are symmetric to A and B, respectively), see the black curves in Fig. 3(c). In detail, the current from stack A (whose tapes turn into the normal state at ~ 1.1 s, see Fig.3(c)), penetrates stack B from the bottom, which is however heating up. Thus, the current from the bottom tapes is passed to the top (colder) tapes in stack B, which is carrying its current and part of that from stack A. Nevertheless, eventually also stack B turns into the normal state and the current is forced to go from the top tapes, through the stack, into the core, see the blue curves in Fig. 3(c), which becomes the only current carrier once the stacks are quenched.

2) Temperature evolution

The evolution of the temperature in the stacks at the beginning of the quench propagation, i.e., when the current is still partially flowing in the stacks, is driven by the current distribution in the stabilizer (copper) of the tapes. Since most of the current has flown from the bottom to the - still superconducting - top tapes in stack A, when the stacks turn into the normal state, most of the current is still in the top tapes. Thus, it is forced to go to the stabilizer of the top tapes, before passing to the bottom tapes (again) and then to the core. Therefore, between $t = 0.9$ s and $t = 1.1$ s, there is more current in the stabilizer of the top tapes than of the bottom tapes. In turn, the heat generation in the top part of stack A is larger, leading to higher temperature in that part of the stack, as represented by the reddish curves in Fig. 4. The same is true for stack B, in which,
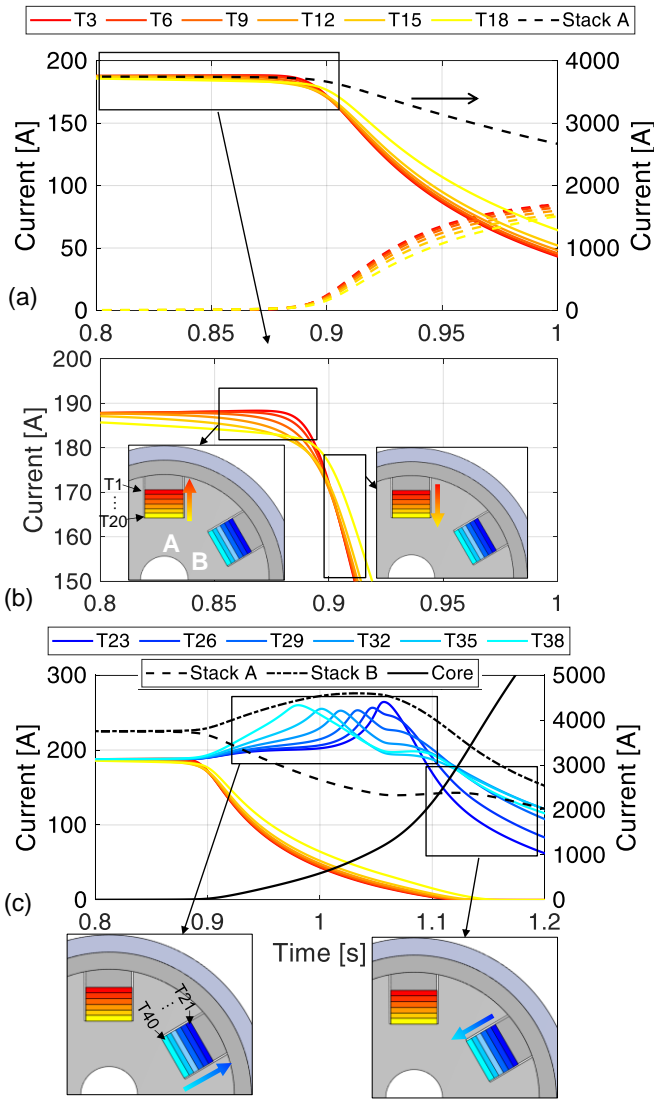
Fig. 3. Evolution of the current in selected tapes in (a) stack A and in (c) stacks A and B (left axes). (b) Zoom of the evolution of the current in the superconducting layers of Stack A. The evolution of the current in the superconductor and stabilizer of the selected tapes is shown with solid and dashed lines, respectively, in (a). The evolution of the total current in selected stacks and in the core is also shown (right axes). The transverse redistribution of the current in each slot is shown schematically with arrows in the sketch of the sample cross-section.

after $t \sim 0.95$ s, the temperature in the top tapes rises faster than in the bottom part of the stack.

B. Comparison of the three samples

The computed evolution of the hot-spot temperature in the three samples is reported in Fig. 5(a). The behavior is quite different and it stems from the different orientation (and distribution) of the tapes. C2 stacks have a higher T_{CS} than the B-D stacks in C1 and B-E and C-F stacks in C3, thus the current sharing starts later. This leads to a slightly higher hot-spot temperature, as already observed in the case of a quench induced at the maximum margin location, i.e. where the T_{CS} is highest, in LTS conductors [27]. Indeed, with the same conditions of the
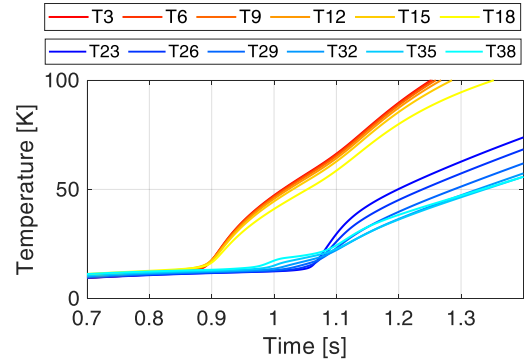

Fig. 4. Evolution of the temperature of selected tapes in stacks A and B.

other two samples, the quench in C2 is detected 0.5 s later, leading to a slightly higher hot-spot temperature than C3.

On the other hand, the tapes arrangement in C3 is advantageous for the current redistribution with respect to C1, because the top tapes are closer to the core, thus the current can be shared more easily between and the stacks. This leads to a lower hot-spot temperature with respect to C1.

The quench front is defined as the position where the temperature of the tape is equal to the local T_{CS}. Therefore, in C1 and C3, where the T_{CS} is not the same for all the slots, the quench starts propagating first in the slots where the T_{CS} is lower and after less than 0.5 s it starts propagating in the other slots, as expected. On the other hand, the quench front propagation is very similar within the tapes of the same slot. To allow a fair comparison of the quench front propagation in the three configurations, the top tape of slot A is examined. As it can be seen from Fig. 5(b), the quench fronts start propagating upstream with respect to the position where the magnetic field is maximum, x_{Bmax}, because of the heating induced by the hot helium entering the CICC. At the beginning, the propagation is quite fast, until the fronts reach the region where the magnetic field decreases, causing a slowing down of the front propagation. The normal region then starts shrinking when the current goes from the stacks to the core, because the local T_{CS} progressively increases. Nevertheless, the temperature in the stacks is high and it is more convenient for the current to flow in the core than to go back in the stacks.

The results obtained for the quench of the three samples support the following requirements for the sample instrumentation:

- more than one temperature sensor in the conductor cross-section, at least one close to the stacks and one on the jacket, are needed in order to capture the temperature gradients on the cross-section, in the region where the quench is expected to initiate;
- at least one voltage tap inside the conductor cross-section is needed in order to quantify the possible voltage differences in the same cross-section among, e.g., the core and the stacks and/or the jacket;
- at least one temperature sensor and one voltage tap are needed on the conductor jacket, every 10 cm along the
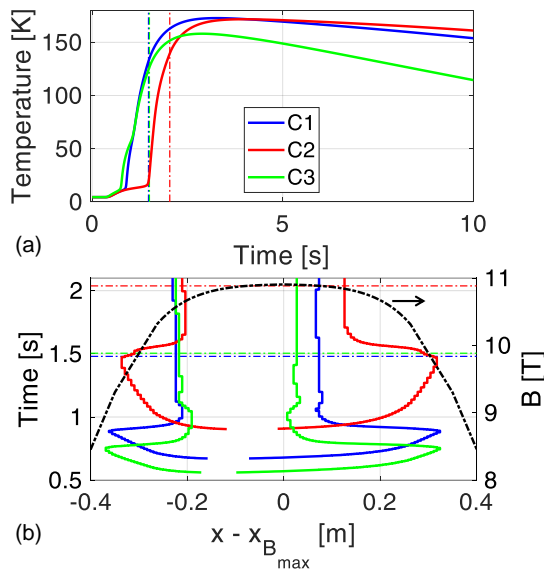
Fig. 5. (a) Evolution of the hot-spot temperature, and (b) propagation of the quench front in tape T1 of C1, C2 and C3. The corresponding dump times are also reported (dash-dotted lines). The magnetic field profile is shown in black in (b). The evolutions are synchronized at the start of the warm He entrance (t = 0 s).

CICC in the maximum field region, see Fig. 5(b), in order to (electrically and thermally) capture the quench propagation.

VI. Conclusions and perspective

The design of several HTS CICC samples to be tested in SULTAN is ongoing at ENEA. A 1D thermal-hydraulic/electric model of the samples has been developed here using the H4C code to support their design as well as to contribute to the definition of the SULTAN diagnostics layout.

The model has also helped understanding how the current should redistribute in the conductor cross-section.

The data to be collected in SULTAN during the forthcoming quench experiments of the C1-C3 samples in 2021 will be extremely helpful for the validation of the H4C model presented in this paper.

References

[1] W. H. Fietz, C. Barth, S. Drotziger, W. Goldacker, R. Heller, S. I. Schlachter, and K. P. Weiss, "Prospects of high temperature superconductors for fusion magnets and power applications," *Fusion Engineering and Design*, vol. 88, no. 6-8, 2013.

[2] L. Rossi, A. Badel, M. Bajko, A. Ballarino, L. Bottura, M. Dhalle,´ M. Durante, P. Fazilleau, J. Fleiter, W. Goldacker, E. Har¨o, A. Kario, ¨G. Kirby, C. Lorin, J. Van Nugteren, G. De Rijk, T. Salmi, C. Senatore, A. Stenvall, P. Tixador, A. Usoskin, G. Volpini, Y. Yang, and N. Zangenberg, "The EuCARD-2 future magnets European collaboration for accelerator-quality HTS magnets," *IEEE Transactions on Applied Superconductivity*, vol. 25, no. 3, 2015.

[3] D. Larbalestier, A. Gurevich, D. Feldmann, and A. Polyanskii, "High-tc superconducting materials for electric power applications," *Nature*, vol. 414, no. 6861, pp. 368–377, 2001.

[4] A. Morandi, M. Fabbri, B. Gholizad, F. Grilli, F. Sirois, and V. M. R. Zermeno, "Design and Comparison of a 1-MW/5-s HTS SMES With ˜

[5] M. Parizh, Y. Lvovsky, and M. Sumption, "Conductors for commercial mri magnets beyond nbti: Requirements and challenges," *Superconductor Science and Technology*, vol. 30, no. 1, 2017.

[6] P. Bruzzone, W. H. Fietz, J. V. Minervini, M. Novikov, N. Yanagi, Y. Zhai, and J. Zheng, "High temperature superconductors for fusion magnets," *Nuclear Fusion*, vol. 58, no. 10, 2018.

[7] T. Mulder, J. Weiss, D. Van Der Laan, A. Dudarev, and H. T. Kate, "Recent Progress in the Development of CORC Cable-In-Conduit Conductors," *IEEE Transactions on Applied Superconductivity*, vol. 30, no. 4, 2020.

[8] M. J. Wolf, W. H. Fietz, M. Heiduk, R. Heller, C. Lange, A. Preuß, and K. P. Weiss, "HTS CroCo - A Strand for High Direct Current Applications," *Journal of Physics: Conference Series*, vol. 1590, 2020.

[9] P. Bruzzone, R. Wesche, D. Uglietti, and N. Bykovsky, "High temperature superconductors for fusion at the Swiss Plasma Center," *Nuclear Fusion*, vol. 57, no. 8, 2017.

[10] G. Celentano, G. De Marzi, F. Fabbri, L. Muzzi, G. Tomassetti, A. Anemona, S. Chiarelli, M. Seri, A. Bragagni, and A. Della Corte, "Design of an industrially feasible twisted-stack HTS cable-in-conduit conductor for fusion application," *IEEE Transactions on Applied Superconductivity*, vol. 24, no. 3, 2014.

[11] M. Takayasu, L. Chiesa, L. Bromberg, and J. V. Minervini, "HTS twisted stacked-tape cable conductor," *Superconductor Science and Technology*, vol. 25, no. 1, 2012.

[12] L. Muzzi, G. De Marzi, A. Di Zenobio, and A. Della Corte, "Cable in-conduit conductors: Lessons from the recent past for future developments with low and high temperature superconductors," *Superconductor Science and Technology*, vol. 28, no. 5, 2015.

[13] R. Heller, P. V. Gade, W. H. Fietz, T. Vogel, and K. . Weiss, "Conceptual Design Improvement of a Toroidal Field Coil for EU DEMO Using High-Temperature Superconductors," *IEEE Transactions on Applied Superconductivity*, vol. 26, no. 4, pp. 1–5, 2016.

[14] Y. Wu and L. Wang, "Anisotropy of the magnetic field of the TF coils in CFETR," *Fusion Engineering and Design*, vol. 143, pp. 240 – 246, 2019.

[15] B. Sorbom, J. Ball, T. Palmer, F. Mangiarotti, J. Sierchio, P. Bonoli, C. Kasten, D. Sutherland, H. Barnard, C. Haakonsen, J. Goh, C. Sung, and D. Whyte, "Arc: A compact, high field, fusion nuclear science facility and demonstration power plant with demountable magnets," *Fusion Engineering and Design*, vol. 100, pp. 378 – 405, 2015.

[16] K. Sedlak, V. A. Anvar, N. Bagrets, M. E. Biancolini, R. Bonifetto, F. Bonne, D. Boso, A. Brighenti, P. Bruzzone, G. Celentano, A. Chiappa, V. D'Auria, M. Dan, P. Decool, A. Della Corte, A. Dembkowska, O. Dicuonzo, I. Duran, M. Eisterer, A. Ferro, C. Fiamozzi Zignani, W. H. Fietz, C. Frittitta, E. Gaio, L. Giannini, F. Giorgetti, F. Gom¨ory, ¨X. Granados, R. Guarino, R. Heller, C. Hoa, I. Ivashov, G. Jiolat, M. Jirsa, B. Jose, R. Kembleton, M. Kumar, B. Lacroix, Q. Le Coz, M. Lewandowska, A. Maistrello, N. Misiara, L. Morici, L. Muzzi, S. Nicollet, A. Nijhuis, F. Nunio, C. Portafaix, G. Romanelli, X. Sarasola, L. Savoldi, B. Stepanov, I. Tiseanu, G. Tomassetti, A. Torre, S. Turtu, D. Uglietti, R. Vallcorba, L. Viererbl, M. Vojenciak, C. Vorpahl, ˋK. P. Weiss, R. Wesche, M. J. Wolf, L. Zani, R. Zanino, A. Zappatore, and V. Corato, "Advance in the conceptual design of the European DEMO magnet system," *Superconductor Science and Technology*, vol. 33, no. 4, 2020.

[17] R. Heller, P. Blanchier, W. H. Fietz, and M. J. Wolf, "Quench analysis of the HTS crossconductor for a toroidal field coil," *IEEE Transactions on Applied Superconductivity*, vol. 29, no. 7, 2019.

[18] A. Zappatore, R. Heller, L. Savoldi, M. J. Wolf, and R. Zanino, "A new model for the analysis of quench in HTS cable-in-conduit conductors based on the twisted-stacked-tape cable concept for fusion applications," *Superconductor Science and Technology*, vol. 33, no. 6, 2020.

[19] R. Kang, D. Uglietti, R. Wesche, K. Sedlak, P. Bruzzone, and Y. Song, "Quench Simulation of REBCO Cable-in-Conduit Conductor With Twisted Stacked-Tape Cable," IEEE Transactions on Applied Superconductivity, vol. 30, no. 1, pp. 1–7, jan 2020.

[20] A. Zappatore, W. Fietz, R. Heller, L. Savoldi, M. Wolf, and R. Zanino, "A critical assessment of thermal-hydraulic modeling of HTS twisted-stacked-tape cable conductors for fusion applications," *Superconductor Science and Technology*, vol. 32, no. 8, 2019.

[21] A. Zappatore, A. Augieri, R. Bonifetto, G. Celentano, L. Savoldi, A. Vannozzi, and R. Zanino, "Modeling quench propagation in the ENEA HTS cable-in-conduit conductor," *IEEE Transactions on Applied Superconductivity*, vol. 30, no. 8, 2020.

Toroidal and Solenoidal Geometry," *IEEE Transactions on Applied Superconductivity*, vol. 26, no. 4, pp. 1–6, 2016.

[22] P. Bruzzone, B. Stepanov, R. Wesche, M. Bagnasco, F. Cau, R. Herzog, M. Calvi, M. Vogel, M. Jenni, M. Holenstein and H. Rajainmaki, "Status Report of the SULTAN Test Facility," *IEEE Transactions on Applied Superconductivity*, vol. 20, no. 3, pp. 455-457, 2010.

[23] W. H. Fietz, N. Bagrets, R. Heller, L. Savoldi, K. P. Weiss, M. J. Wolf, R. Zanino, and A. Zappatore, "Determination of the thermal resistance between pressed copper-copper and copper-stainless steel interfaces for high current HTS CICC," presented at Magnet Technology conference, Vancouver, Canada, 2019.

[24] Y. Cengel, R. Turner, and R. Smith, "Fundamentals of Thermal-Fluid Sciences," *Applied Mechanics Reviews*, 2001.

[25] T. L. Bergman, A. S. Lavine, F. P. Incropera, and D. P. Dewitt, Fundamentals of Heat and Mass Transfer. John Wiley & Sons, 2011.

[26] Z. Piątek, B. Baron, T. Szczegielniak, D. Kusiak and A. Pasierbek, "Mutual inductance of two thin tapes with parallel widths," *Przegląd Elektrotechniczny*, vol. 89, pp. 281-283, 2013.

[27] L. Savoldi, R. Bonifetto, R. Zanino, and L. Muzzi, "Analyses of Low and High-Margin Quench Propagation in the European DEMO TF Coil Winding Pack," *IEEE Transactions on Plasma Science*, vol. 44, no. 9, pp. 1564– 1570, 2016.